Maghrebian Journal of Pure and Applied Science
ISSN : 2458-715X
http://revues.imist.ma/?journal=mjpas&page=index

QSAR studies on 2-arylethenylquinoline derivatives as multifunctional agents for the treatment of Alzheimer's disease via CoMFA and CoMSIA analysis

K. Dguigui[1*]. M. Lahmouad[2*], N.N. Mrabti [1*], M. Errajy [1], M. El Hallaoui[1]

[1] Equipe de chimie informatique et modélisation, Laboratoire d'ingenieurie des matériaux, de modélisation et d'environnement, LIMME, Faculté des sciences Dhar El Mehraz, Université Sidi Mohammed Ben Abdellah, USMBA, BP. 1796, 30000, Atlas, Fès. Maroc.
[2] University Caddy Ayad, Faculté of Médecine and pharmacie, Marrakech. Maroc

***Corresponding Author; Email:** dguiguikhalid@gmail.com (Dguigui Khalid)
Mery.lah0136@gmail.com (Lahmouad Meriem)

Received 14 April 2019, Revised 30 December 2019, Accepted 20 April 2020

Abstract: Comparative molecular field analysis (CoMFA) and comparative molecular similarity indices analysis (CoMSIA) were applied to the potential multifunctional agents for the treatment of Alzheimer's disease (AD). Predictive 3D-QSAR models were established using Sybyl-x 2.0 multifit molecular alignement rule over a training set and test set. The optimum models were all statistically significant with cross-validated coefficients (Q2)> 0.6 and conventional coefficients (R2)>0.9, indicating that they were reliable enough for activity prediction. The obtained results may aid in the desing of novel bioactive quinoline derivatives.
Keywords: Alzheimer's disease (AD), CoMFA and CoMSIA.).

1.Introduction

Alzheimer's disease (AD) is an age-related neurodegenerative brain disease that affects more than 24 million older people worldwide, with the number of patients expected to reach 70 million by 2050 [1]. The pathogenesis of AD is not fully understood, and multiple factors have been suggested to contribute to the development of AD, such as low levels of acetylcholine, β-amyloid (AB) deposits, tau protein aggregation and oxidative stress, there are still no effective drugs that could prevent the progression of AD. Given these factors, small molecules have been widely discovered, but so far only acetylcholinesterase (AChE) inhibitors and the N-methyl-D-aspartate receptor antagonist (NMDA), memantine, have been approved for clinical use [2]. Compounds that may interact with two or more Alzheimer's disease targets have become of great interest in the treatment of Alzheimer's disease in recent years.

Following the work of wq and his colleague's .In the present study we have made a theoretical study. , we are attempt to establish 3D-QSAR (three-dimensional quantitative structure activity relationship) analysis of these 2-arylethenylquinoline derivatives by using comparative molecular field analysis CoMFA and comparative molecular similarity indices analysis CoMSIA [3] approach for extracting a correlation between biological activity and chemical structure(4), therefore, predict models and evaluate what structural features (hydrogen bond donor/Acceptor, hydrophobic, steric and electrostatic) are responsible for this inhibition of self induced $A_{\beta 1\text{-}42}$ aggregation. Whilst, Toropova build up a model QSAR of gamma secretase inhibitors using the montecarlo methods.

2.Materials and methods

2.1. Data set

All 2-arylethenylquinoline derivatives and their $A_{\beta 1-42}$ aggregation inhibition were collected from literature(1), the Aβ1-42 values were converted into the corresponding $pA_{\beta 1-42}$ (-log $A_{\beta 1-42}$). (Table 1)

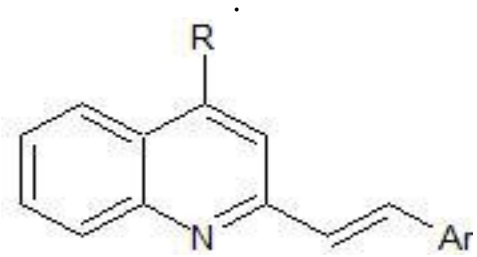

Figure 1. 2-arylethenylquinoline derivatives

Table1. 2-arylethenylquinoline derivatives and their observed and predicted $A_{\beta 1-42}$ activities

Compounds	Substituent's		Experimental activity		Predicted activity	
	R	Ar	$A_{\beta 1-42}$	p $A_{\beta 1-42}$	CoMFA	CoMSIA
1	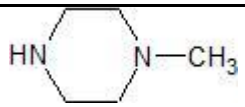	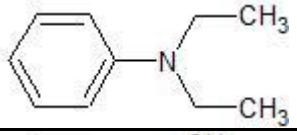	85.2	1.93	1.88	1.88
2	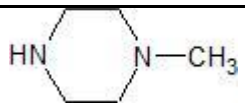	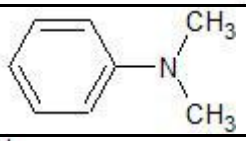	79.5	1.90	1.85	1.86
3	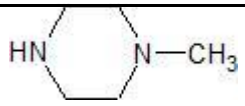	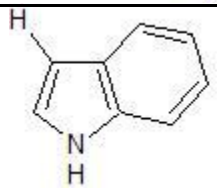	79.3	1.89	1.87	1.87
4	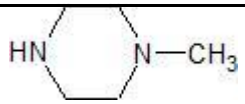	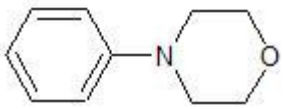	72.1	1.85	1.83	1.85
5	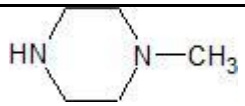	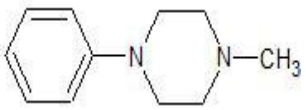	59.0	1.77	1.74	1.75
6	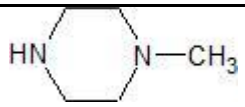	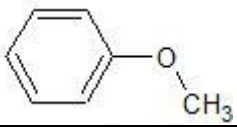	57.4	1.75	1.75	1.76
7	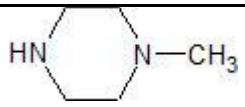	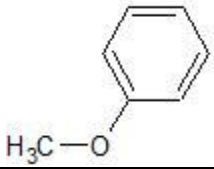	54.4	1.73	1.74	1.75
8	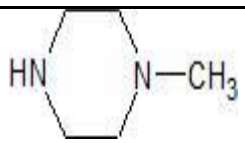	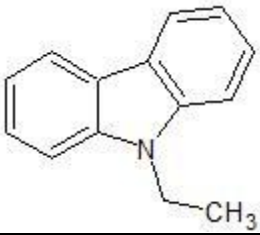	51.8	1.71	1.69	1.70

9	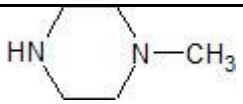		74.3	1.87	1.83	1.83
10	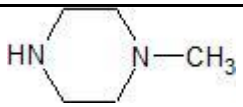	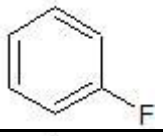	49.93	1.69	1.69	1.69
11	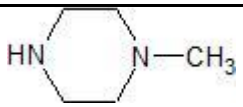	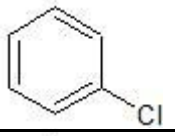	38.9	1.58	1.57	1.58
12	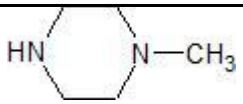	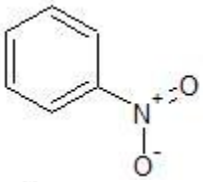	28.5	1.45	1.48	1.48
13	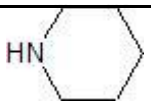	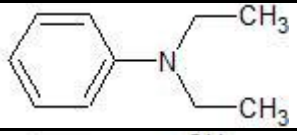	85.8	1.93	1.93	1.93
14		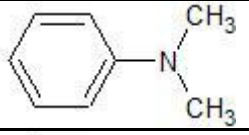	84.0	1.92	1.90	1.90
15	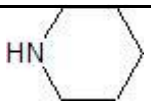	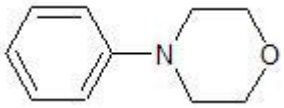	77.7	1.89	1.88	1.89
16	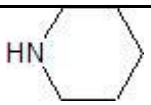	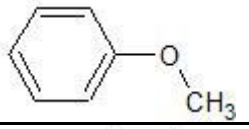	67.0	1.82	1.80	1.80
17	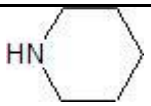	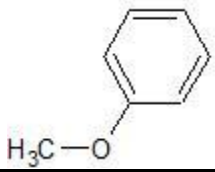	63.6	1.80	1.79	1.79
18	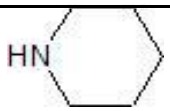	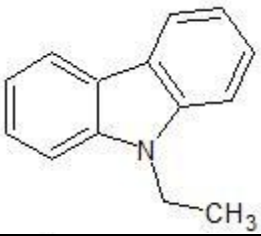	59.3	1.77	1.74	1.74
19	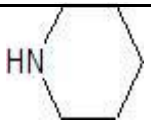	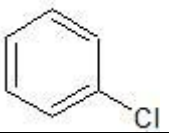	41.8	1.62	1.63	1.62
20	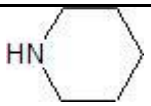	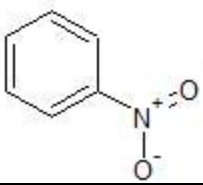	38.2	1.58	1.53	1.53

21	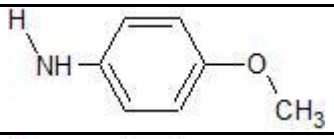	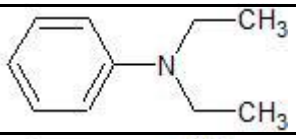	80.3	1.90	1.90	1.91
22	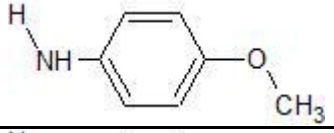	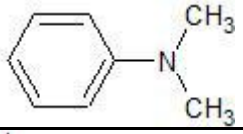	79.9	1.90	1.88	1.88
23	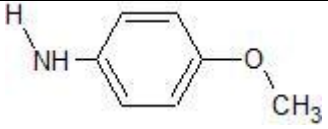	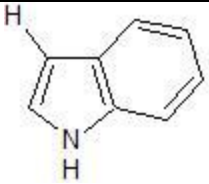	81.2	1.91	1.89	1.90
24	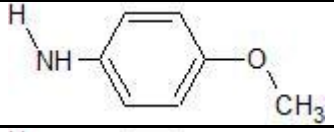	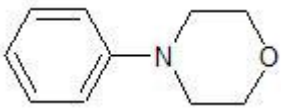	79.5	1.80	1.86	1.87
25	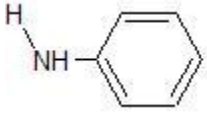	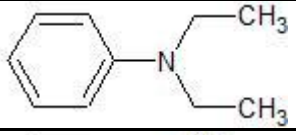	77.3	1.88	1.89	1.90
26	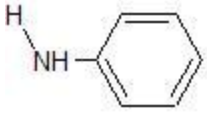	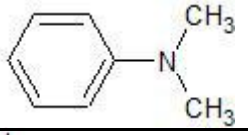	76.8	1.89	1.86	1.87
27	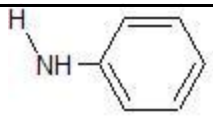	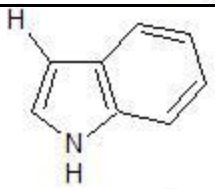	78.1	1.89	1.88	1.89
28	H	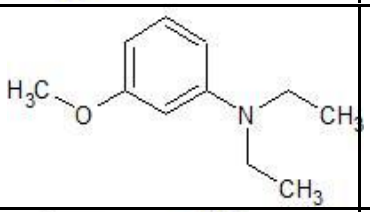	62.8	1.79	1.68	1.68
29	H	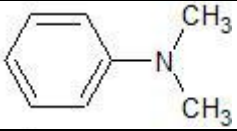	53.9	1.73	1.74	1.75
30	H	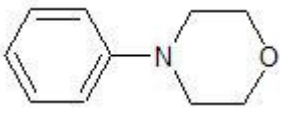	57.9	1.76	1.73	1.74
31	H	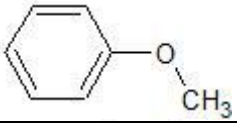	48.8	1.69	1.70	1.70
32	H	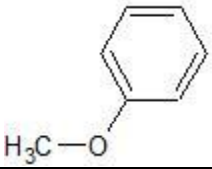	47.9	1.68	1.63	1.63

33	H	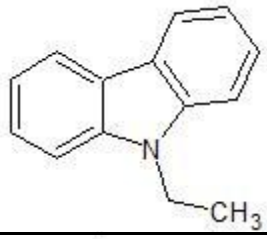	43.2	1.63	1.59	1.60
34	H	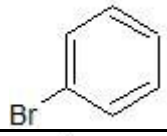	44.8	1.65	1.68	1.68
35	H	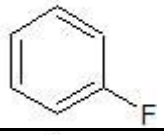	40.0	1.60	1.58	1.58
36	H	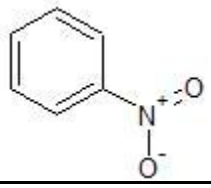	23.8	1.37	1.38	1.38

2.2. Molecular alignment

A good alignment is the most essential for the quality and the predictive ability of CoMFA and CoMSIA models. Thus, we applied molecular alignment using align database-rigid body alignment of molecules in a Mol 2 database with a user defined common core of sybyl-x (5) in present study. The most active compound 13 was selected as the template molecule and the other molecules were aligned onto it by common substructure wild bold lines as shown in figure 1. It can be seen that all the studied compounds have similar minimum conformation.

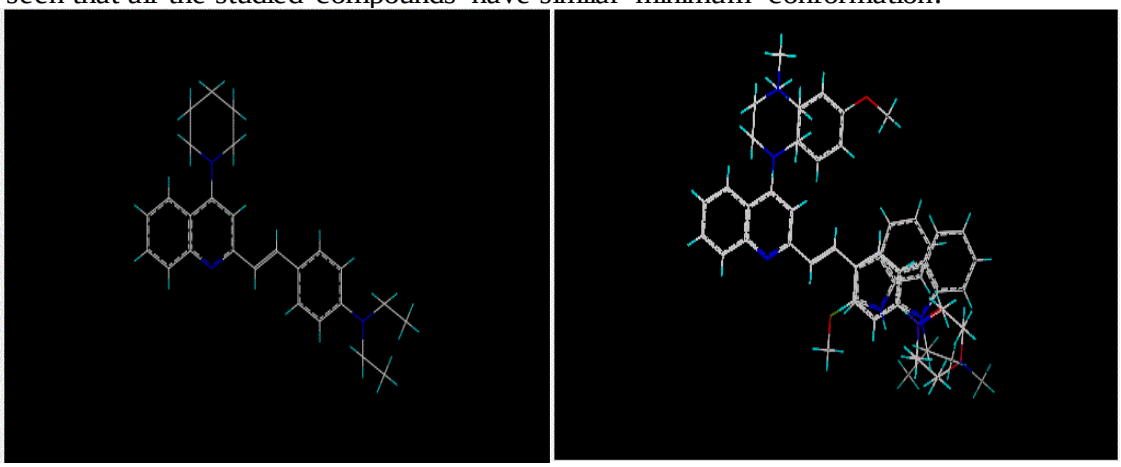

(a) (b)

Figure 1. (a) template used for molecular alignment of set inhibitors (compound 13), (b) Molecular alignment

2.3. 3D-QSAR modeling generation

CoMFA

Steric and electrostatic potential fields for CoMFA were calculated at each lattice intersection of a regularly spaced grid box. Lattice spacing was set to a value 2.0 A in all X, Y, and Z directions. An sp^3 carbon atom with a charge of +1.0 served as the probe atom to calculate steric and electrostatic fields. The cut-off was set to 30 Kcal/mol (sybyl default energy cutoff). Cross validated regression coefficient (Q^2) values were calculated by using partial the least-squares

(PLS) methodology [6]. Leave-one-out [7] cross validation was used to obtaine optimum number of components [7].

CoMSIA

In CoMSIA study, by using a sp^3 carbon atom probe with a charge of +1.0, five similarity indices consisting of steric (S), electrostatic (E), hydrophobic (H), hydrogen bond donor (D) and acceptor (A) field were calculated for each lattice with a grid of 2.0 A. the optimal number of components was designated such that cross –validated was maximal and standard error of prediction was minimal.

PLS Analysis

Partial least squares (PLSs) regression [8], with the leave-one-out (LOO) cross-validation procedure was carried out to determine the optimal number of components [9. 10]. The cross validated coefficient Q^2, as an internal statistical index of predictive power, was subsequently obtained. Q^2 is calculated according to the formula [11].

$$Q^2 = 1 - \frac{\sum (Y_{obs} - Y_{CVpred})^2}{\sum (Y_{obs} - Y_{mean})^2} \qquad (1)$$

Where Y_{mean} means average activity value of the entire data set, while Y_{obs} , Y_{pred} and Y_{CVpred} represent observed predicted and cross-validated activity values, respectively. Often, a high Q^2 and R^2 value ($Q^2 > 0.6$, $R^2 > 0.7$) is considered as a proof of high predictive ability of the model(12) .

The CoMFA and CoMSIA results were graphically interpreted by field contribution maps using field type" STDEV*COEFF" and the contour levels were set to default values.

3.Results and discussion

3.1. *CoMFA analysis*

The statistical parameters of the CoMFA and CoMSIA models are given in table 1. The best CoMFA model showed the cross-validated coefficient Q^2 of 0.91 with a number of components N=9, and standard Error of 0.022629. The field contributions of steric and electrostatic were 0.124 and 0.704. The correlation between the predicted and experimental activity is shown in figure 2, (CoMFA model).

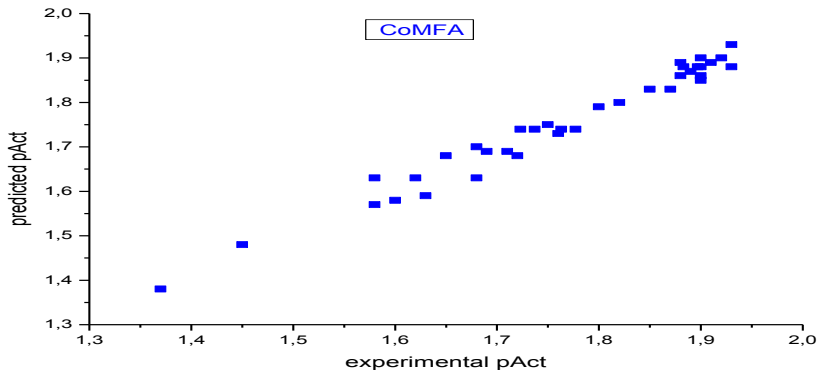

Figure 2. *CoMFA model*

All of the values indicated the CoMFA model had a satisfactory statistical correlation (R^2= 0.98) and a well predictive activity (all statistical of CoMFA by PLS method are reported in table 2.

Table 2. CoMFA Model

Model name	Q^2	R^2	SEE N
CoMFA	0.91	0.98	0.02269

Q^2= the leave-one-out (LOO) cross-validation coefficient; R^2= the predictive correlation coefficient; SEE= standard error of estimate; N= optimum number of components constructs the model.

3.2. *CoMSIA analysis*

CoMSIA descripting the five fields (SEHDA: Steric, Electrostatic, Hydrophobic, Hydrogen-bond Donor and Acceptor fields) played significant roles in the prediction of inhibition of self-induced Aβ1-42 aggregation activity. The predicted activity values for the set were listed in table 1, and depicted graphically in figure 3.

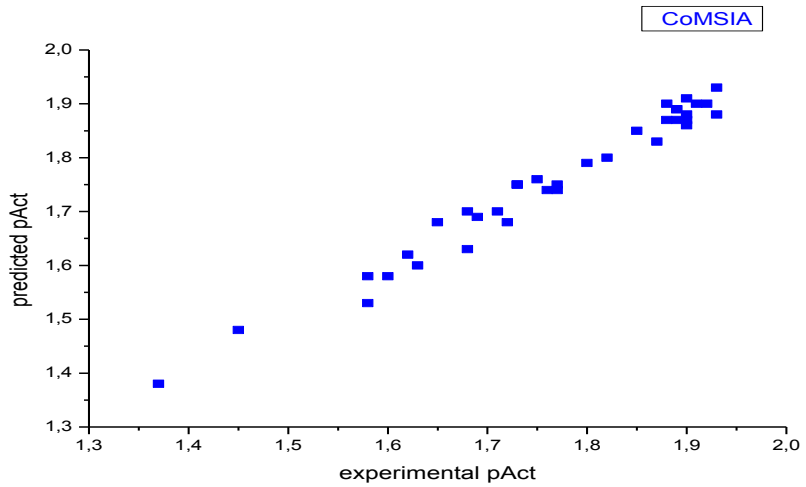

Figure 3. CoMSIA model

Table 3. CoMSIA Model

Model name	Q^2	R^2	SEE N
CoMSIA	0.91	0.98	0.0225 10

Q^2= the leave-one-out (LOO) cross-validation coefficient; R^2= the predictive correlation coefficient; SEE= standard error of estimate; N= optimum number of components.

The high Q^2, R^2 along with low SEE value, indicated a good statistical correlation and reasonable predictability of the CoMSIA model.

3.3. *External validation*

One cannot judge the predictability of the developed model from internal validation for an entirely new set of compounds, as internal validation considers the chemicals belonging to the same set of compounds used for model development. Thus for external validation, the available data set is usually divided in to training and test sets, then subsequently a model is developed with the training set, and then the constructed model is employed to check the external validation employing the test set molecules which are not utilized in the model development process. The external validation ensures the predictability and applicability of developed QSAR model for the prediction of untested molecule (13).

In this study, we devised the data set into training set (n=30) and test set (n=6) and we have obtained the results presented in the table 4.

Table 4. External validation

Model name	Q^2	R^2	Q^2 TEST	R^2 TEST	Q^2 TRAINING	R^2 TRAINIG
CoMFA	0.91	0.981	0.89	0.95	0.87	0.94
CoMSIA	0.911	0.982	0.89	0.96	0.87	0.94

The high Q^2_{TEST}, R^2_{TEST}, $Q^2_{TRAINING}$, $R^2_{TRAINIG}$, indicated a good statistical model and reasonable predictability of 3D-QSAR model.

3.4. CoMFA contour maps

The steric and electrostatic contour maps of the CoMFA models are shown in figure 4. Compound 13 was used as the reference molecule and displayed in the map in aid of visualization. The CoMFA contour maps results were graphically interpreted by field contribution using the STDEV*COEFF field type [14].

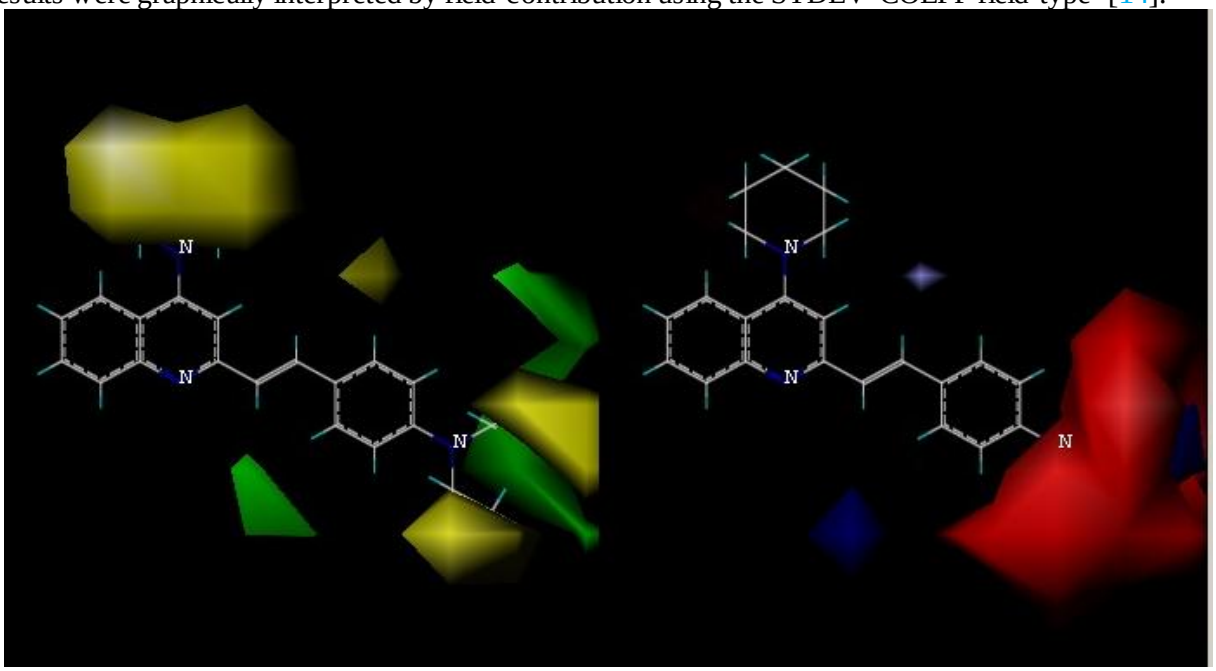

Figure 4. contour maps of CoMFA: steric and electrostatic based on compound 13

The green contours represent desirable steric bulk, where bulky substituent's (alkyl amino group) would increase the activity, while the yellow contours represent regions where the steric bulky group (aromatic amino group) would be undesirable, else, the blue and red contours depict the position where positively charged groups and negatively charged groups would be favourable [15].

The CoMFA steric contour maps showed three green contours at 2- position aryl substituent. This indicate that bulky substituent is preferred in this region to produce higher inhibition of self induced $A_{\beta 1-42}$ aggregation activity, which explain why compounds 1, 13, 14 with alkyl amino group and aromatic amino group had well activity than compounds with methoxy group on the aromatic amino group at the 4-position of quinoline ring (21, 22, and 23 compounds) contributed to increased activity [16].

4.Conclusion

In conclusion, QSAR-CoMFA/CoMSIA analysis was applied to the new 2-arylethenylquinoline derivatives as multifunctional anti Alzheimer agents. Majority of compounds displayed high effective inhibitory potencies against $A_{\beta 1-42}$ aggregation. CoMFA and CoMSIA models with good predictive capabilities were obtained and used for prediction of against self induced $A_{\beta 1-42}$; also, by CoMFA and CoMSIA we can show that the introduction of suitable electron-donating group in phenyl ring is crucial to the inhibitory 158 potency of the compounds against self induced CoMSIA descripting aggregation.

REFERNCES

1. Wang X-Q, Xia C-L, Chen S-B, Tan J-H, Ou T-M, Huang S-L. Design, synthesis, and biological evaluation of 2-arylethenylquinoline derivatives as multifunctional agents for the treatment of Alzheimer's disease. **Eur J Med Chem. 7 janv;89:349‑61 (2015).**

2. Sharma R, Dhingra N, Patil S. CoMFA, CoMSIA, HQSAR and Molecular Docking Analysis of Ionone-based Chalcone Derivatives as Antiprostate Cancer Activity. **Indian J Pharm Sci. 1 janv;78:54 (2016).**
3. Yp L, X W, Fx N, Jb O, Jq H, Hb L, et al. 3D-QSAR studies of azaoxoisoaporphine, oxoaporphine, and oxoisoaporphine derivatives as anti-AChE and anti-AD agents by the CoMFA method. **J Mol Graph Model. 16 ;41:61‑7 (2013).**
4. Wu S, Qi W, Su R, Li T, Lu D, He Z. CoMFA and CoMSIA analysis of ACE-inhibitory, antimicrobial and bitter-tasting peptides. **Eur J Med Chem. 12;84:100‑6 (2014).**
5. SYBYL-X 2.1 | Scientific Computing World, (**2020**).
6. Myint KZ, Xie X-Q. Recent Advances in Fragment-Based QSAR and Multi-Dimensional QSAR Methods. **Int J Mol Sci. 8;11(10):3846‑66 (2010).**
7. Wold S. Cross-Validatory Estimation of the Number of Components in Factor and Principal Components Models. **Technometrics. 1; 20(4): 397‑405 (1978).**
8. Tyagi C, Gupta A, Goyal S, Dhanjal JK, Grover A. Fragment based group QSAR and molecular dynamics mechanistic studies on arylthioindole derivatives targeting the α-β interfacial site of human tubulin. **BMC Genomics. 8;15(9):S3 (2014).**
9. Peng, Li J, Wang J, Zhang X, Zhai H. Investigations of FAK inhibitors: a combination of 3D-QSAR, docking, and molecular dynamics simulations studies. **J Biomol Struct Dyn. 26;36(6):1529‑49 (2018).**
10. Dguigui K, Elhallaoui M. 3 D-QSAR Modeling of Substituted Thiophene-Anthranilamides as Potent Inhibitors of Human Factor XA Using Quantum Chemical Descriptors. (**2015**).
11. Roy K, Kar S, Das RN. A Primer on QSAR/QSPR Modeling: Fundamental Concepts [Internet]. Springer International Publishing; janv (**2020**).
12. Das RN, Sintra TE, Coutinho JAP, Ventura SPM, Roy K, Popelier PLA. Development of predictive QSAR models for Vibrio fischeri toxicity of ionic liquids and their true external and experimental validation tests. **Toxicol Res;5(5):1388‑99 (2016).**
13. Cheng P, Li J, Wang J, Zhang X, Zhai H. Investigations of FAK inhibitors: a combination of 3D-QSAR, docking, and molecular dynamics simulations studies. **J Biomol Struct Dyn; 36(6):1529‑49 (2018).**
14. Kakarla P, Inupakutika M, Devireddy AR, Gunda SK, Willmon TM, Ranjana K, et al. 3D-qsar and contour map analysis of tariquidar analogues as multidrug resistance protein-1 (mrp1) inhibitors. **Int J Pharm Sci Res;7(2):554‑72 (2016).**
15. Jihan Hameed Abdulameer. (PDF) Synthesis and Characterization of Nickel, Palladium, Platinum and Cupper with New Oxazipine Ring. (**2020**).
16. Kharkar, Prashant S.; Reith, Maarten E. A.; Dutta, Aloke K. structure-activity relationship 3d-qsar: Topics by WorldWideScience.org. (***2008***).